

Intelligent Control for Doubly Fed Induction Generator Connected to the Electrical Network

Anass Bakouri, Hassane Mahmoudi, Ahmed Abbou

Department of Electrical Engineering, Mohammed V University, Mohammadia School of Engineers Rabat, Morocco

Article Info

Article history:

Received Nov 12, 2015

Revised Mar 12, 2016

Accepted Apr 13, 2016

Keyword:

ANN

DFIG

DTC

WECS

ABSTRACT

In this paper we are interested in optimizing the wind power capture, using the Doubly Fed Induction Generator (DFIG). This machine is preferred to other types of variable speed generator because of their advantages in economic terms and control. The Artificial Neural Network (ANN) based on Direct Torque Control (DTC) which is used to control the electromagnetic torque in order to extract the maximum power. The main objective of this intelligent technique is to replace the conventional switching table by a voltage selector based on (ANN) to reduce torque and flux ripples. Moreover, the fuzzy logic controller is used to grid side converter to keep DC link voltage constant, and also to achieve unity power factor operation. The main advantage of the two control strategies proposed in this paper is that they are not influenced by the variation of the machine parameter. The pitch control is also presented to limit the generator power at its rated value. Simulation results of 1,5 MW, for (DFIG) based Wind Energy Conversion System (WECS) confirm the effectiveness and the performance of the global proposed approaches.

*Copyright © 2016 Institute of Advanced Engineering and Science.
All rights reserved.*

Corresponding Author:

Anass Bakouri,

Department of Electrical Engineering, Mohammed V University,

Mohammadia School of Engineers, Morocco.

Email: Anass.Bakouri@gmail.com

1. INTRODUCTION

In recent years, renewable energy and cutting carbon emissions have become on the top of the global environmental agenda, many buildings are able to use alternative energy sources to meet a substantial portion of their energy demands and to reduce dependence on imported fossil fuels in order to make energy production more sustainable. Renewable energy can be produced from a wide variety of sources including wind, solar, hydro, tidal and geothermal. The main goal is to conserve the environment through generating clean, it also drives technological innovation and employment across the world. The wind turbine generator system is one of the fastest growing energy technologies in the world which is a clean source of energy that produces no air or water pollution.

Doubly fed induction generator (DFIG) is a very popular machine which is used for variable-speed systems where the speed range requirements are small, for example $\pm 30\%$ of synchronous speed, due to the many advantages offer over other types of generators, such as reduced inverter cost, because inverter rating is typically 25% of total system power, reduced cost of the converter and filters, because filters are rated for 0.25 p.u. total system power, and converter harmonics represent a smaller fraction of total system harmonics that improves system efficiency [1] [2], therefore operates in both sub- and super-synchronous modes with a rotor speed range around the synchronous speed. The most configuration used in wind energy conversion that the stator circuit is directly connected to the grid while the rotor winding is connected via slip-rings to a three-phase converter [3]. In order to get a satisfactory power output of wind turbines, control strategies are also needed to be developed on the basis of control strategies that have been previously obtained.

The power converter is comprised of the rotor-side converter (RSC) and the grid-side converter (GSC) in which the rotor side converter (RSC) is controlled in the aim to follow the optimal electromagnetic torque in order to extract the maximal wind power available, while the grid side converter controls the DC-link voltage and regulate the power factor at unit [4].

Firstly direct torque control (DTC) has been considered as a solution to many challenges of classical methods, such as field oriented control (FOC) and vector control (VC), these classic methods require precise information of the machine parameters, such as rotor, stator, the resistance of the inductance and the mutual inductance [5, 6, 7]. Thus the performance is assigned when the real machine parameters differ from those used values in the control system because the gains of the PI controllers are constant. Using hysteresis controllers instead of conventional PI controllers in the DTC control leads to good performance despite the machine parameters variation. The major problem which associated with the basic DTC scheme lies in the high flux and torque ripples due to the variable switching frequency. The direct power control (DPC) is proposed in [89 10] this technique is based on the principles of DTC, the optimal voltage vectors is selected from a pre-defined switching table which depends on errors value between the reference and estimated values of active and reactive power, and the angular position. These classical methods focuses on the use of PI regulations (FOC, VC) their robustness is affected with the machine parameter variations and the major problem of direct controls (DTC, DPC) is the variable switching frequency that will affect the quality of power injected into the network.

However, this paper proposes an intelligent and advanced control which is based on a combination of Artificial Neural Network (ANN), it also based on Direct Torque Control (DTC) technique applied in RSC and fuzzy logic control to control the GSC, this approach of control significantly reduces the ripples of electromagnetic torque and the flux, improve the quality of the power and also gives high performance in presence of variations in parameters of the machine.

The paper is arranged as follows: section-2 the modeling of all systems presented. Section-3 and 4 describes the proposed system and the control scheme. In section-5 simulation results and discussion are given. Finally a conclusion is presented.

2. WECS MODELLING

2.1. Wind Turbine Model

Thanks to the turbine, the kinetic energy of wind is converted into mechanical power, the mechanical torque developed by the wind turbine is expressed by [11] [12]:

$$T_w = \frac{P_w}{\Omega_t} = \frac{C_p(\lambda, \beta) \rho \pi R^2 V_w^3}{2\Omega_t} \quad (1)$$

where $C_p(\lambda, \beta)$ is the power coefficient, V_w is the wind speed (m/s), R is the radius of the turbine disk, ρ is the air density, Ω_t is the turbine speed, λ is the tip speed ratio and β is the pitch angle. The power coefficient of C_p is expressed by (1), it depends of the turbine characteristics (λ tip speed ratio and β blade pitch angle) [13]. The Figure 1 illustrates the curves of the power coefficient versus λ for different values of β , for each pitch angle, there is one specific optimal tip-speed-ratio λ_{opt} at which C_p takes a maximum value and the wind turbine is most efficient.

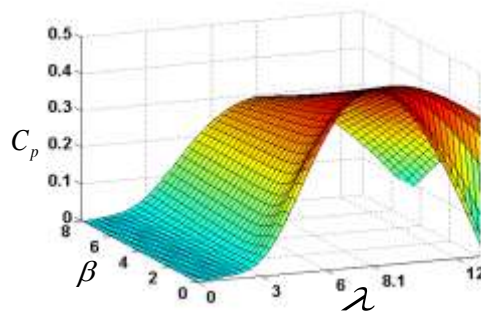


Figure 1. The power coefficient variation C_p against tip speed ratio λ and pitch angle β

$$C_p(\lambda, \beta) = 0.5176 \left(\frac{116}{\lambda_i} - 0.4\beta - 5 \right) \exp\left(-\frac{21}{\lambda_i}\right) + 0.0068\lambda \quad (2)$$

where λ and λ_i are given by:

$$\begin{cases} \frac{1}{\lambda_i} = \frac{1}{\lambda + 0.08\beta} - \frac{0.035}{\beta^3 + 1} \\ \lambda = \frac{R\Omega_t}{V_w} \end{cases} \quad (3)$$

2.2. Transmission Elements Model

The fundamental principle of the dynamics is applied to know the evolution of the mechanical speed.

$$J \frac{d\Omega_m}{dt} = T_m - T_{em} - f \Omega_m \quad (4)$$

where J and f are the system moment of inertia and the friction coefficient respectively. Figure 2 shows wind generator power curves at various, and Figure 3 shows the mathematical model of the mechanical part of the wind turbine with MPPT algorithm.

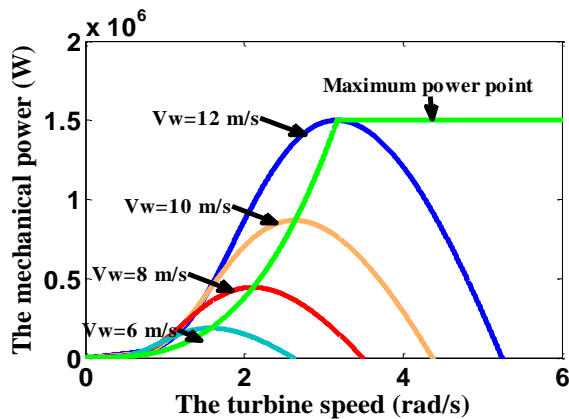


Figure 2. Wind generator power curves at various

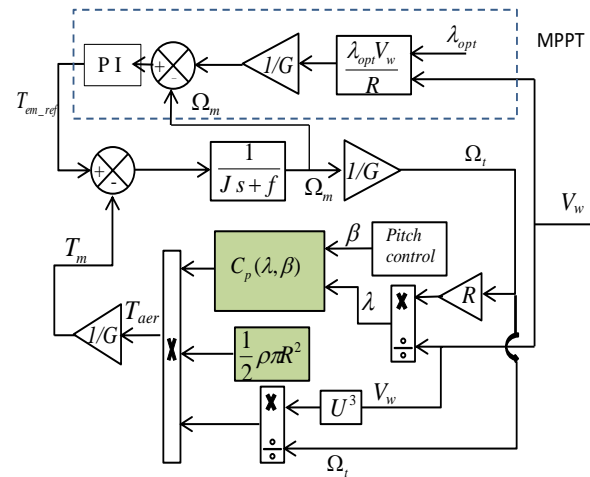


Figure 3. Wind turbine model with the wind speed MPPT algorithm

2.3. Maximum Power Point Tracking (MPPT) and Pitch Control

In order to capture the maximum power of the incident wind, we must adjust the rotational speed of the turbine permanently to the winds. The optimum operation speed of the generator is estimated by the following equation:

$$\Omega_{m-opt} = \frac{\lambda_{opt} \cdot V_w}{R} \quad (5)$$

λ_{opt} and Ω_{m-opt} are the tip speed ratio and the rotor speed optimal respectively. The Figure 2 shows the MPPT curve where the power extracted is maximized. The MPPT operation mode aims to maximize power extraction for medium and low wind speeds by following the maximum power point curve (C_{p-max}) as depicted in Figure 2. We have to maintain the tip speed ratio at its optimal value, $C_p = 0.48$ and

β should be equal to 0, to extract the maximum power, to achieve these objectives; the speed of the DFIG is controlled using the electromagnetic torque, to follow the optimum rotational speed.

For the high wind speeds, the wind power captured by the wind turbine which exceeds rated value allowed, for safety and efficiency reasons, the wind turbines are subject to operating limits this limitation is typically achieved by using pitch angle control. The purpose of pitch control is to maintain the optimum blade angle to limit the power produced at its rated value in order to protect the wind turbine. For low and medium wind speed, the pitch control is inactivated and the output of PI controller equal to 0 which means that $\beta = 0$, where the switch is in position 1, in the opposite case the switch is moved to position 2 (the pitch control is activated).

The block diagram of pitch angle system is shown in Figure 4 where P_{rated} and P_g are the rated power and the generator power respectively.

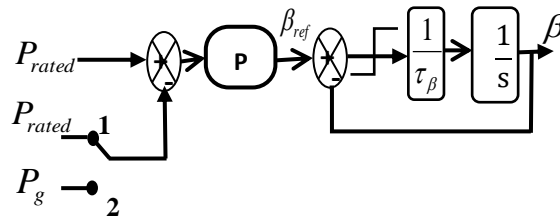


Figure 4. The Block of pitch angle

2.4. Modeling of the DFIG

The DFIG is described in the Park d-q frame by the following set of equations [14] [11].

$$\begin{cases} V_{sd} = R_s i_{sd} + \frac{d\phi_{sd}}{dt} - \omega_s \phi_{sq} \end{cases} \quad (6)$$

$$\begin{cases} V_{sq} = R_s i_{sq} + \frac{d\phi_{sq}}{dt} + \omega_s \phi_{sd} \end{cases} \quad (7)$$

$$\begin{cases} V_{rd} = R_r i_{rd} + \frac{d\phi_{rd}}{dt} - \omega_r \phi_{rq} \end{cases} \quad (8)$$

$$\begin{cases} V_{rq} = R_r i_{rq} + \frac{d\phi_{rq}}{dt} + \omega_r \phi_{rd} \end{cases} \quad (9)$$

$$\begin{cases} \phi_{sd} = L_s i_{sd} + L_m i_{rd} \end{cases} \quad (10)$$

$$\begin{cases} \phi_{sq} = L_s i_{sq} + L_m i_{rq} \end{cases} \quad (11)$$

$$\begin{cases} \phi_{rd} = L_r i_{rd} + L_m i_{sd} \end{cases} \quad (12)$$

$$\begin{cases} \phi_{rq} = L_r i_{rq} + L_m i_{sq} \end{cases} \quad (13)$$

where $\phi_{sd}, \phi_{sq}, \phi_{rd}, \phi_{rq}, i_{sd}, i_{sq}, i_{rd}, i_{rq}$ are the fluxes and currents of the stator and rotor in (dq) axes, R_r and R_s are the resistances of the rotor and stator windings, L_s, L_r and L_m are the stator, rotor, and mutual inductances respectively.

2.5. Model of the Converters

The converter model is expressed by the two following equations:

$$\begin{bmatrix} V_{sa} \\ V_{sb} \\ V_{sc} \end{bmatrix} = \frac{V_{dc}}{3} \begin{bmatrix} -2 & 1 & 1 \\ 1 & -2 & 1 \\ 1 & 1 & -2 \end{bmatrix} \begin{bmatrix} S_a \\ S_b \\ S_c \end{bmatrix} \quad (14)$$

$$i_{dc} = S_a i_a + S_b i_b + S_c i_c \quad (15)$$

(Sa, Sb, Sc) are logic variables which represent the switch states obtained by the application of the proposed control. i_{dc} and V_{dc} are the current and direct bus voltage respectively. DC link voltage model is given by [15]:

$$P_r = CV_{dc} \frac{dV_{dc}}{dt} + P_g \quad (16)$$

where P_r is the active power of rotor-side power converter, P_g is the active power of the grid-side power converter and C is the capacitance.

2.6. Filter Model

The connection of the GSC to the electrical network is realized out via an RL filter in order to reduce the harmonics frequency generated from power converter commutations. The model of the filter is given by [16]:

$$\begin{bmatrix} V_{f1} \\ V_{f2} \\ V_{f3} \end{bmatrix} = R_f \begin{bmatrix} i_{f1} \\ i_{f2} \\ i_{f3} \end{bmatrix} + L_f \frac{d}{dt} \begin{bmatrix} i_{f1} \\ i_{f2} \\ i_{f3} \end{bmatrix} + \begin{bmatrix} V_{g1} \\ V_{g2} \\ V_{g3} \end{bmatrix} \quad (17)$$

The Park transformation of equation (17) gives the following equations:

$$V_{fd} = R_f i_{fd} + L_f \frac{di_{fd}}{dt} - L_f \omega_e i_{fq} + V_{gd} \quad (18)$$

$$V_{fq} = R_f i_{fq} + L_f \frac{di_{fq}}{dt} + L_f \omega_e i_{fd} + V_{gq} \quad (19)$$

where R_f and L_f are the filter resistance and filter inductance respectively, i_{fd} and i_{fq} are the currents of d-axis and q-axis which crossing the filter respectively, V_{fq} and V_{fd} are the filter voltage of q-axis and d-axis respectively, V_{gd} and V_{gq} are the grid voltage components of d-axis and q-axis respectively, and ω_e is the grid frequency.

3. DTC PRINCIPLE OF DFIG

The direct control strategy has many advantages, a simplest structure, the fast dynamic response, reliability and lowerparameter dependency [17], but it has some drawbacks, such as the torque and flux ripple. To overcome this kind of problem, we have applied in this work an DTC based on artificial neural network (DTC-ANN), it is an improvement of the classical DTC. In the following, we define the equations that will be used in the proposed control scheme. The α and β estimates of the Rotor flux ϕ_r vector are :

$$\begin{cases} \phi_r = \int_0^t (V_{r\alpha} - R_r i_{r\alpha}) dt \\ \phi_r = \int_0^t (V_{r\beta} - R_r i_{r\beta}) dt \end{cases} \quad (20)$$

The module and the phase of the rotor flux are given by:

$$\begin{cases} \phi_r = \sqrt{\phi_{r\alpha}^2 + \phi_{r\beta}^2} \\ \theta_r = \arctg \frac{\phi_{r\beta}}{\phi_{r\alpha}} \end{cases} \quad (21)$$

The electromagnetic torque equation of the DFIG in stationary reference frame is a function of the rotor, the stator fluxes and the angle (ϕ_r, ϕ_s) [18]:

$$T_{em} = \frac{3}{2} P \frac{L_m}{\sigma L_r L_s} |\phi_r| |\phi_s| \sin \delta \tag{22}$$

where $\sigma = 1 - \frac{L_m^2}{L_r L_s}$ is the leakage coefficient and δ is the angle between the space vectors of the stator and rotor flux. According to this equation we can notice that the torque depends on the rotor and stator flux amplitudes and also the angle δ between the space vectors. The stator flux space vector were created in the machine that has constant amplitude because the stator of the DFIG is connected to a balanced grid, by controlling the angle and the rotor flux amplitude; it is possible to control the electromagnetic torque so that it has the desired value which allows us to extract the maximum power.

When the vector of rotor flux is in zone i, the control of the electromagnetic torque and the rotor flux can be obtained by selecting one of the eight vectors following the information presented in Figure 5. Depending on the value of the torque error, the output of the hysteresis regulator (3-level), Figure 6 K_{Tem} can take a value of 1, -1, or 0 which mean increase, decrease, or keep the value of electromagnetic torque. Similarly, depending on the flux error, the output of the hysteresis regulator (two-level), Figure 6 can take only a value of 0 or 1 which mean increase or decrease of the rotor flux.

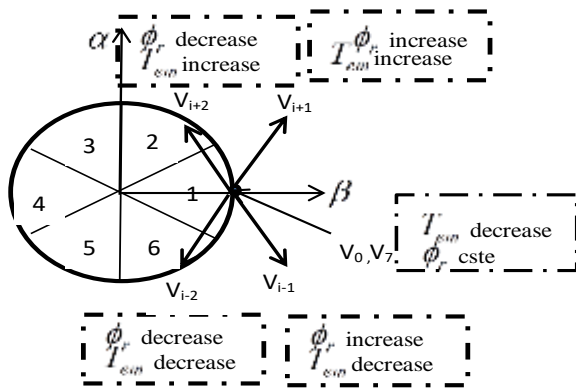


Figure 5. Detection of vector voltage

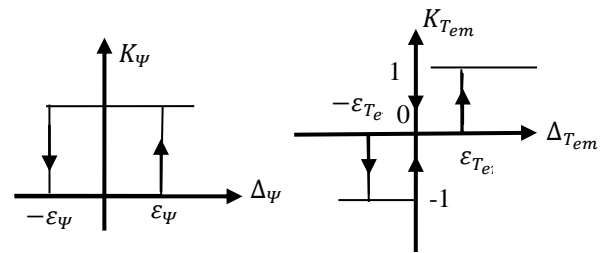


Figure 6. Levels hysteresis regulator for torque and flux

The control Table 1 allows choosing the adequate vector according the output value of the hysteresis regulator and the sector where the rotor flux space vector is located.

Table 1. Switching Table

Sector		1	2	3	4	5	6
KΨ	KTem						
KΨ=1	KTem=1	V2	V3	V4	V5	V6	V1
	KTem=0	V7	V0	V7	V0	V7	V0
	KTem=-1	V6	V1	V2	V3	V4	V5
KΨ=0	KTem=1	V3	V4	V5	V6	V1	V2
	KTem=0	V0	V7	V0	V7	V0	V7
	KTem=-1	V5	V6	V1	V2	V3	V4

3.1. The Neural Network Selector

Artificial neural networks have been gaining a lot of attention in the recent years. In machine learning domain, ANN's are a family of mathematical models inspired from biological neural networks. It is an approach which gives more possibilities to address the problems of memory, perception, learning

and analysis in new ways [19] [17]. A feedforward neural network is organized in layers: an input layer, one or more hidden layers and an output layer. The backpropagation algorithm is the best-known learning algorithm for multilayer networks.

In this work, the intelligent technique has based on Artificial Neural Network which was used to replace the classical switching table by the neural network selector in order to reduce torque ripple and flux. The inputs of the ANN selector block are the position of rotor flux vector represented by a number of sectors and the outputs of the hysteresis comparator for the torque and rotor flux. The outputs of this block are the impulses that allowing the control of the inverter switches (Sa, Sb, Sc).

The control scheme of the proposed DTC based on Artificial Neural Network for a DFIG system which is illustrated in Figure 7. The Network that has taken in this application is a 3-5-1 feed forward network Figure 8 where the first layer is from a log sigmoid transfer function, hidden layer is hyperbolic tangent sigmoid transfer function and the third layer (output) is of linear transfer function. The training method used was Levenberg-Marquardt back-propagation

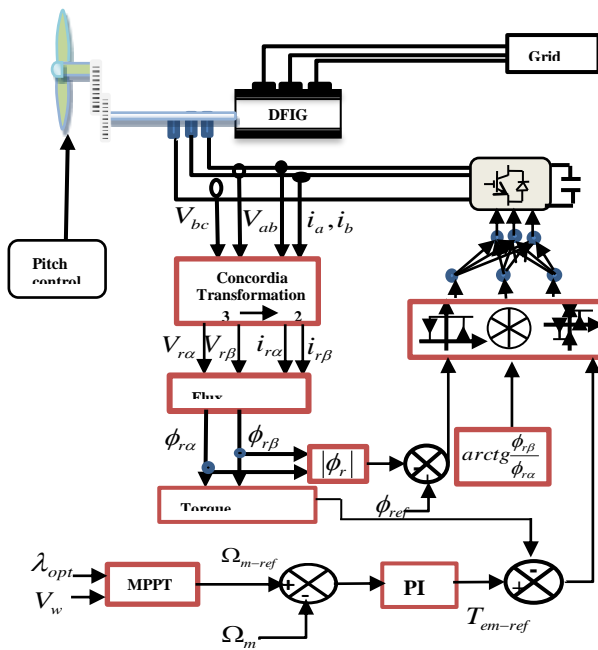


Figure 7. Schematic diagram of the control DTC based

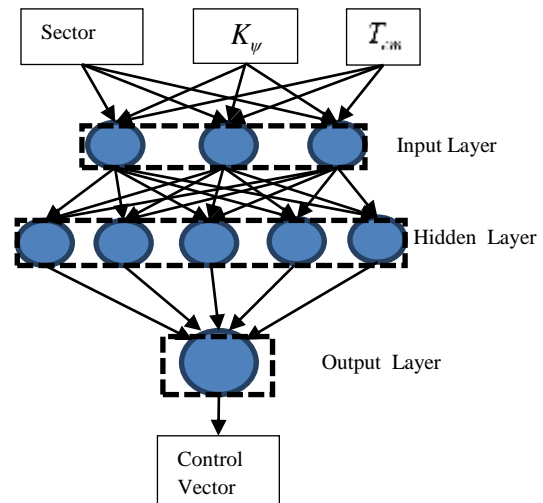


Figure 8. Feed Forward NN for sector selection on ANN for a DFIG

4. CONTROL OF THE GRID SIDE CONVERTER (GSC)

The control system presented in this part is based on fuzzy logic controller (FLC) is selected mainly for two reasons: The first one, it does not need any mathematical model of the process under control and the second one, is simple and easy for practical implementations, it is able to give a very satisfactory performance to control the grid side converter of DFIG in order to inject the power produced by the rotor into the network with unit power factor and regulating the DC bus at a desired value. The reactive power Q and active power Pg flows are respectively expressed as follow:

$$\begin{cases} P_g = \frac{3}{2}(v_{gd}i_{gd} + v_{gq}i_{gq}) \\ Q_g = \frac{3}{2}(v_{gd}i_{gq} - v_{gq}i_{gd}) \end{cases} \quad (23)$$

The grid voltage space vector is aligned along the D-axis, we obtain

$$\begin{cases} V_{gq} = 0 \\ V_{gd} = V_g \end{cases} \quad (24)$$

The reactive and active power exchanged with an electrical network which can be expressed after orientation by equation (25), consequently we can control the active power by the d-axis current and reactive power by the q-axis current, and the reference values of quadratic current and direct current components can be expressed respectively as follow equations (26):

$$\begin{cases} P_g = V_g i_{fd} \\ Q_g = V_g i_{fq} \end{cases} \tag{25}$$

$$\begin{cases} i_{fd-ref}^* = \frac{P_{g-ref}}{v_g} \\ i_{fq-ref}^* = \frac{Q_{g-ref}}{v_g} \end{cases} \tag{26}$$

We generate the reference of active power by regulating the direct bus voltage with a fuzzy logic controller generating the current reference i_{c-ref} to the capacity Figure 9. Thus, we can express p_{ref} as:

$$P_{ref} = V_{dc} (i_{dc} - i_{c-ref}) \tag{27}$$

$$P_{ref} = P_{dc} - P_{c-ref} \tag{28}$$

with:

$$i_{c-ref} = FLC(V_{dc-ref} - V_{dc}) \tag{29}$$

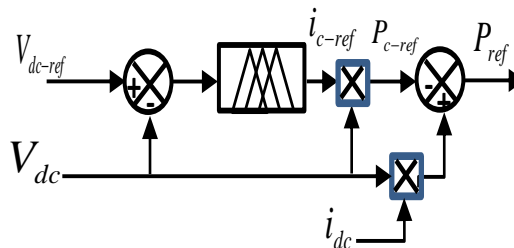


Figure. 9. DC bus control bloc diagram

Substituting (24) in (18) and (19) gives:

$$\begin{cases} V_{fd} = e_d - \overbrace{L_f \omega_e i_{fq}}^{V_{fq}^{comp}} + V_g \\ V_{fq} = e_q + \overbrace{L_f \omega_e i_{fd}}^{V_{fd}^{comp}} \end{cases} \tag{30}$$

where

$$\begin{cases} e_d = R_f i_{fd} + L_f \frac{di_{fd}}{dt} \\ e_q = R_f i_{fq} + L_f \frac{di_{fq}}{dt} \end{cases} \tag{31}$$

Figure 10 shows the Fuzzy logic controller where E_p and E_q are the current errors and $(\int E_p$ and $\int E_q)$ the integration of current errors are used as inputs to the FLC. We added to the output of the FLC, the terms coupling in order to generate the rotor reference voltages that applied to the grid side converter. Seven fuzzy sets are chosen for all input and output which are (positive small) PS, (positive medium) PM (positive big) PB, (zero) Z, (negative big) NB, (negative medium) NM and (negative small) NS.

Three independent FLCs are used to control the reactive power that exchanged between the DFIG and the grid and also to control the dc-link voltage V_{dc} . The fuzzy logic controller contains three functional blocks: fuzzification, fuzzy rule base and defuzzification. There are 49 control rules indicated in Table 2: where E_{pq} and $\int E_{pq}$ as the input signals to the FLC, to compute the output of the FLC, the defuzzification uses the center of gravity method for each FLC [20], the overall structure of the fuzzy logic control of grid-side converter is shown in Figure 11.

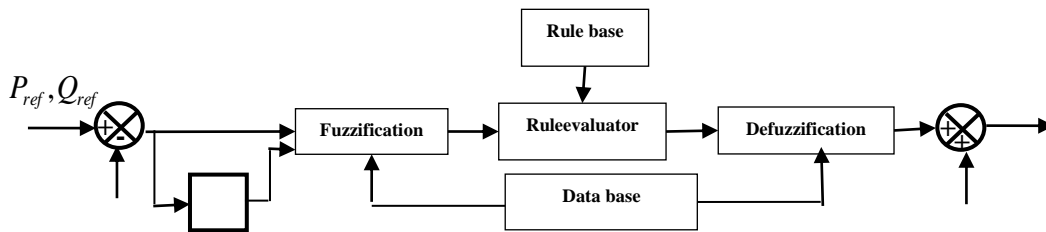


Figure 10. Block diagram of fuzzy controller

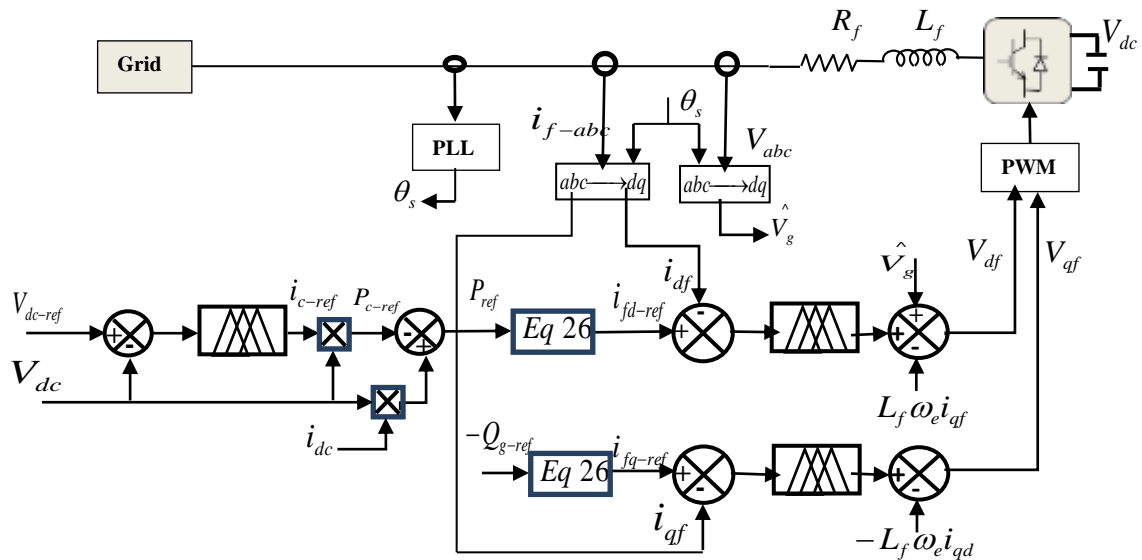


Figure 11. Control block diagram of grid-side converter

5. SIMULATION RESULTS

To check the effectiveness of the proposed control strategies under varying wind speed, simulation studies were performed for a 1.5 MW DFIG-based WECS using Matlab / Simulink software. Figure 12 (a) shows the wind speed profile of DFIG-based WECS. The wind speed varies around the rated wind speed which is 12 m/s. The variation of the wind speed provokes the change of way of functioning in the system. Case 1: The wind turbine operate in the MPPT operating mode, when the wind speed is less than rated speed (12m/s), thus the wind turbine can generate the maximum power according to the specific wind speed. Case 2: For high wind speeds, the pitch control starts operating. Therefore the pitch angle is increased in order to limit the captured wind power to its rated value.

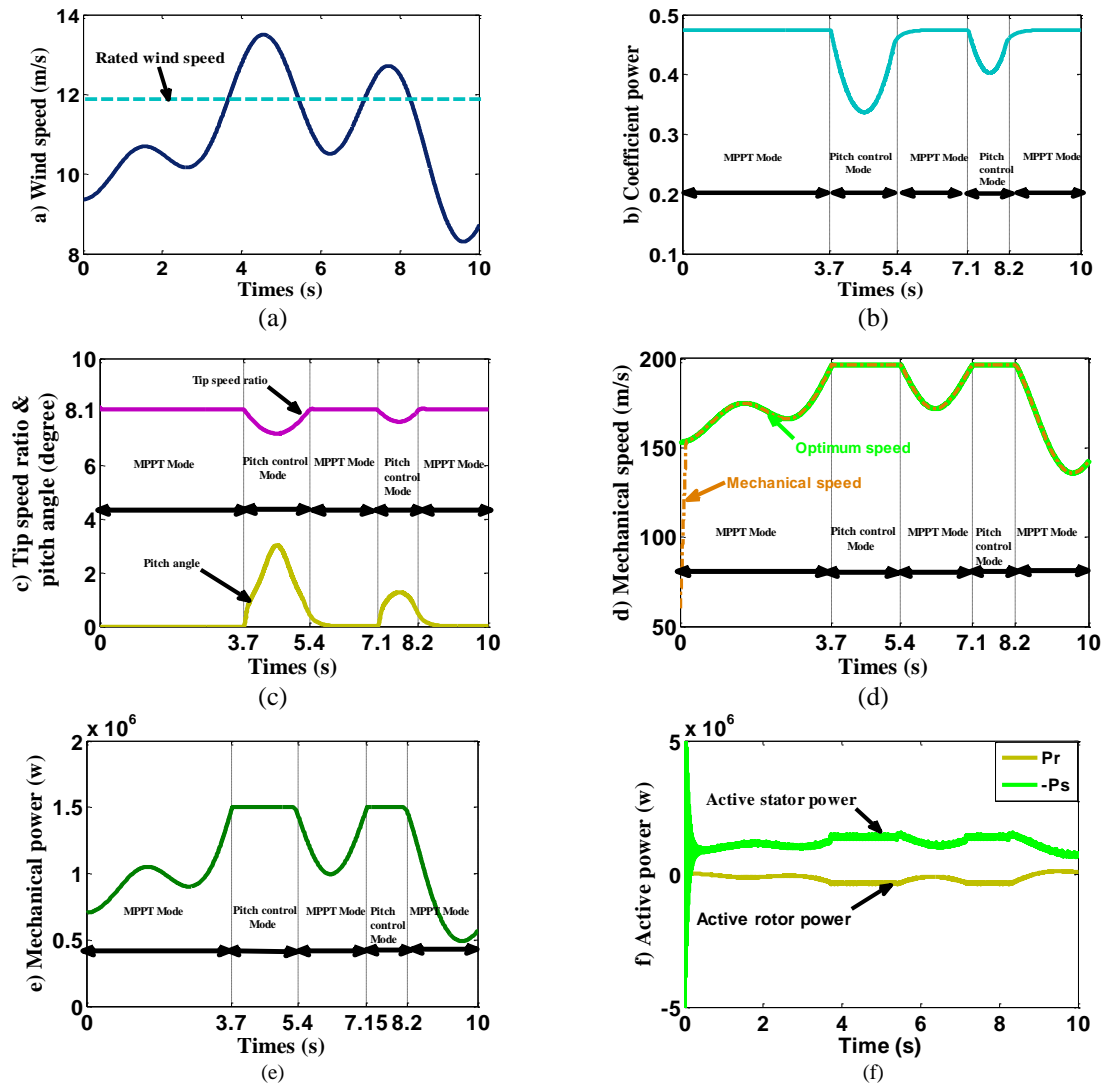


Figure 12. (a) wind speed, (b) Coefficient of performance, (c) tip speed ratio and pitch angle, and (d) Mechanical speed with Optimum speed of reference, (e) Mechanical power, (f) Active stator and rotor power

The Figure 12(b) shows the coefficient power which is equal to $C_p = 0.48$ for MPPT mode and $C_p < 0.48$ for Pitch control mode. The Figure 12(c) shows the tip speed ratio and pitch angle for the MPPT mode $\lambda = 8.1$ and $\beta = 0$, for Pitch control mode $\lambda < 8.1$ and $\beta > 0$, and also the output power is kept at rated value as shown in Figure 12 (e). The Figure 12 (d) shows that the generator speed follow the optimum speed very well. The Figure 12 (f) displays the evolution of the active power of the stator and rotor.

Figure 13(a) and Figure 13(b) show that the electromagnetic torque and the rotor flux follow their reference values respectively. The Figure 13(c) shows that the DC-link voltage is regulated to the reference value fixed at 1400 V. It can be seen that the reactive power is kept at zero value to get the unity power factor operation, as shown in Figure 13 (d).

The robustness of the proposed control strategy is tested by using the variation of the rotor resistance which value used to estimate the rotor flux as shown in (20) is reduced to 20% of its real value. First case (with no variation in parameter of machine): the simulation results are presented in Figure 13 A.

Second case (with 80% rotor resistance error): Figure 13 B shows the simulation results for the same operation conditions as those shown in Figure 13A, but a variation 80% rotor resistance error was applied from the time $t=3$ s to $t=6$ s. By comparing the results of Figure 13A and Figure 13B with and without

variation of rotor resistance, we can observe that there is almost no difference in the result even with a large change in the rotor resistance, the system maintains excellent performance.

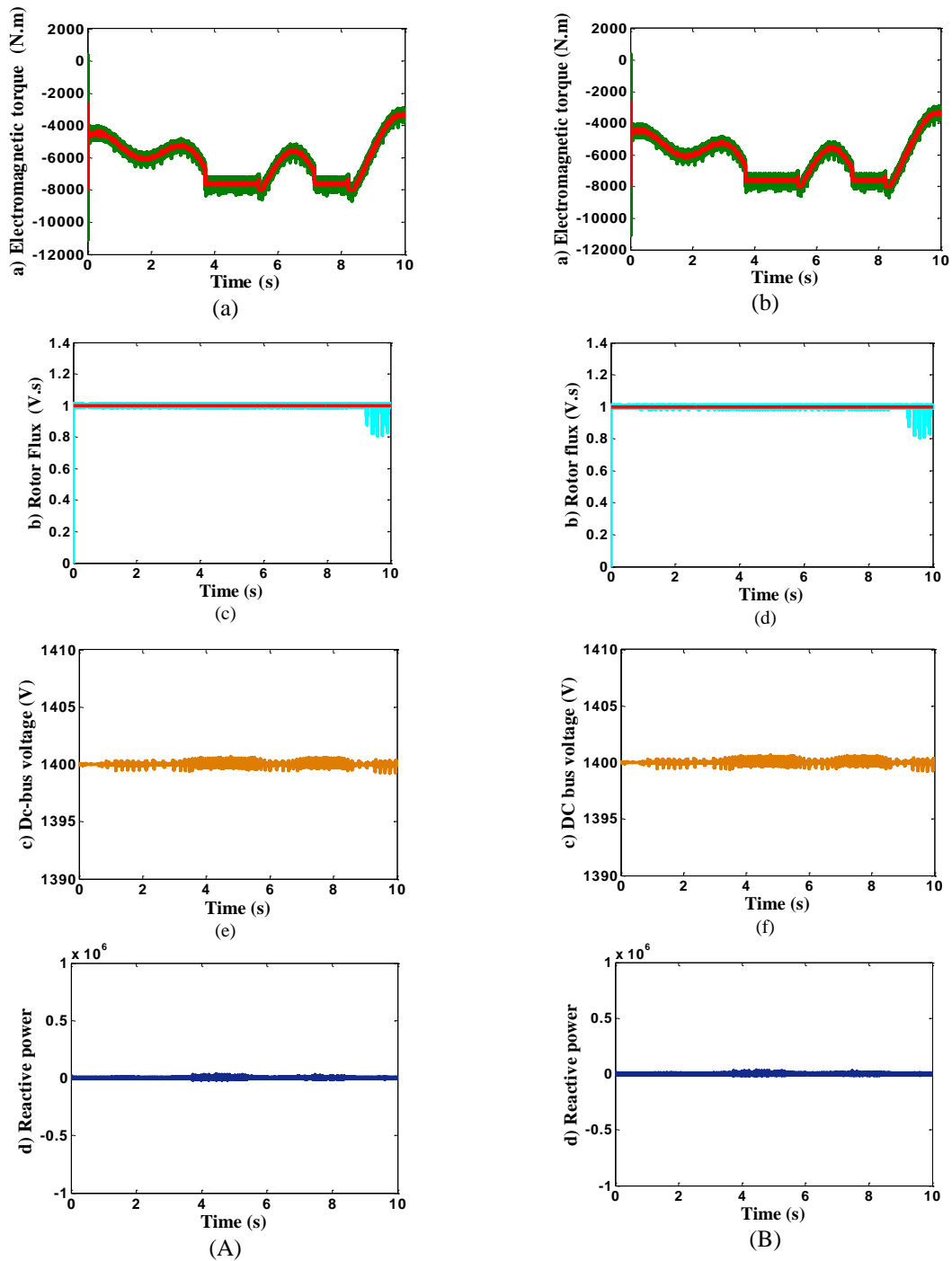


Figure 13. Simulated results (A) without rotor resistance error and (B) with 80% rotor resistance error applied from the time $t=3$ s to $t=6$ s: (a) Electromagnetic torque and its reference, (b) Rotor flux with its reference, (c) Dc-link voltage and (d) Grid reactive power

6. CONCLUSION

A complete system for generating electrical energy is modeled using the DFIG, two control strategies are combined, the first one is a direct torque control strategy which is based on ANN and the second one is the fuzzy logic control. The MPPT method and pitch control are proposed and incorporated in the

control circuit of the power converter to extract the maximum power of the DFIG and also to limit the power at the nominal value for safety reasons. The simulation results are presented to show the effectiveness of the proposed control strategy. It is clear that the fuzzy logic controller gives an excellent performance in terms of regulation of the DC bus voltage and reactive power. The DTC based on ANN reduce greatly the ripple of the torque and flux. The developed models have been implemented using MATLAB/SIMULINK.

APPENDIX

Parameters of machine: $P_n = 1.5$ MW, $f_n = 50$ Hz, $U_n = 690$ V (line–line, rms), Number of pole pairs =2, Stator resistance $R_s = 0.0.0023 \Omega$, Stator leakage inductance: $L_s = 0.00293$ H, Rotor resistance: $R_r = 0.002 \Omega$, Rotor leakage inductance: $L_r = 0.00297$ H, Magnetizing inductance: $L_m = 0.00288$ H.

Table 2. Fuzzy rule table

E_{pq}	$\int E_{pq}$						
	PB	PM	PS	Z	NS	NM	NB
PB	PB	PB	PB	PB	PM	PS	Z
PM	PB	PB	PB	PM	PS	Z	NS
PS	PB	PB	PM	PS	Z	NS	NM
Z	PB	PM	PM	Z	NM	NM	NB
NS	PM	PS	Z	NS	NM	NB	NB
NM	PS	Z	NS	NM	NB	NB	NB
NB	Z	NS	NM	NB	NB	NB	NB

REFERENCES

- [1] S. Müller, M. Deicke, & Rik W. De Doncker Doubly Fed Induction Generator for Wind Turbine a Viable Alternative to Adjust Speed over a wide range at Minimal Cost, *IEEE industry applications magazine*, may-june 2002.
- [2] S. Belfedhal, E. Berkouk, “Modeling and Control of Wind Power Conversion System with a Flywheel Energy Storage System”, *International Journal of Renewable Energy Research, IJRER*, Vol.1, No3, pp. 43-52, 2011.
- [3] John Fletcher and Jin Yang (2010). Introduction to the Doubly-Fed Induction Generator for Wind Power Applications, *Paths to Sustainable Energy*, Dr Artie Ng (Ed.), ISBN: 978-953-307-401-6, InTech, A
- [4] Won-Sang Kim , Sung-Tak Jou , Kyo-Beum Lee and Steve Watkins, “Direct Power Control of a Doudly Fed Induction Generator with a Fixed Switching Frequency”, *Industry Applications Society Annual Meeting*, 2008. IAS '08. IEEE
- [5] I. Takahashi and T. Noguchi, “A new quick-response and high-efficiency control strategy of an induction motor”, *IEEE Trans. Ind. Appl.*, vol. IA-22, no. 5, pp. 820–827, 1986.
- [6] J. Hu and X. Yuan, “VSC-based direct torque and reactive power control of doubly fed induction generator”, *Renewable Energy*, vol. 40, pp 13-23, 2012
- [7] Shuhui Li, Timothy A. Haskew, Rajab Challoo and Marty Nemmers, “Wind Power Extraction from DFIG Wind Turbines Using Stator-Voltage and Stator-Flux Oriented Frames”, *International Journal of Emerging Electric Power Systems*, vol 12, Issue 3, 2011
- [8] Lie Xu, and P. Cartwright, “Direct Active and Reactive Power Control of DFIG For Wind Energy Generation”, *IEEE Transactions On Energy Conversion*, Vol. 21, No. 3, pp.750-758 2006.
- [9] M. Malinowski, M. P. Kazmierkowski, S. Hansen, F. Blaabjerg, and G. D. Marques, “Virtual-flux-based direct power control of three-phase PWM rectifiers”, *IEEE Trans. Ind. Appl.*, vol. 37, no. 4, pp. 1019–1027, Jul.–Aug. 2001.
- [10] G. Escobar, A. M. Stankovic, J. M. Carrasco, E. Galvan, and R. Ortega, “Analysis and design of direct power control (DPC) for a three phase synchronous rectifier via output regulation subspaces”, *IEEE Trans. Power Electron.*, vol. 18, no. 3, pp. 823–830, May 2003.
- [11] Fatma Hachicha and Lotfi Krichen, “Rotor power control in doubly fed induction generator wind turbine under grid faults”, *Energy*. vol. 44, pp. 853-861, 2012.
- [12] E. Muljadi and CP. Butterfield, “Pitch-controlled variable-speed wind turbine generation”, *IEEE transactions on industry applications*, vol. 37, no. 1, january/february 2001.
- [13] Endusa Billy Muhando, Tomonobu Senjyu, Aki Uehara, Toshihisa Funabashi, and Chul-Hwan Kim, “LQG Design for Megawatt-Class WECS With DFIG Based on Functional Model Fidelity Prerequisites”, *IEEE Trans. Energy Conversion*, vol. 24, no. 4, pp. 893-904, Dec. 2009.
- [14] B. Boukhezzer and H. Siguerdidjane, “Nonlinear Control with Wind Estimation of A DFIG Variable Speed Wind Turbine for Power Capture Optimization”, *Energy Conversion and Management*, Vol. 50, pp. 885-892, 2009.
- [15] Nolan D. Caliao, “Dynamic Modeling And Control Of Fully Rated Converter Wind Turbines”, *Renewable Energy*, Vol. 36 pp. 2287-2297, 2011

- [16] H. Li, C. Yanga, B. Zhaoa, H.S. Wanga, and Z. Chen, “Aggregated Models And Transient Performances of A Mixed Wind Farm With Different Wind Turbine Generator Systems”, *Electric Power Systems Research*, Vol. 92, pp. 1– 10, 2012.
- [17] G. Venu Madhav and Y. P. Obulesu, “Direct Torque Control Strategy for Doubly Fed Induction Machine under Low Voltage Dips”, *IJPEDS*, vol.2, no.4, December 2012, pp. 409-416, 2012
- [18] Rajesh Kumar, R.A. Gupta, S.V. Bhangale, Himanshu Gothwal, “Artificial Neural Network Based Direct Torque Control of Induction Motor Drives”, *IET-UK International Conference on Information and Communication Technology in Electrical Sciences (ICTES 2007)*, pp.361-367, 2007
- [19] R. Toufouti, S. Meziane, H. Benalla, “Direct Torque Control For Induction Motor Using Intelligent Techniques”, *Journal of Theoretical and Applied Information Technology*, pp 35-44, 2007
- [20] S. Abdeddaim, A. Betka, “Optimal tracking and robust power control of the DFIG wind turbine”, *Electrical Power and Energy Systems*, Vol. 49, pp 234–242, 2013.